Journal of Groundwater Science and Engineering
ISSN 2305-7068
Indexed by ESCI CABI CSA Scopus GeoRef AJ CNKI

Geothermal anomalies in the Xianshuihe area: Implications for tunnel construction along the Sichuan-Tibet Railway, China

Feng Liu, Wei Zhang, Gui-ling Wang, Shuai-chao Wei, Chen Yue, Guang-zheng Jiang, Yu-zhong Liao

Citation:
Liu F, Zhang W, Wang GL, *et al*. 2023. Geothermal anomalies in the Xianshuihe area: Implications for tunnel construction along the Sichuan-Tibet Railway, China. Journal of Groundwater Science and Engineering, 11(3): 237-248.

View online: https://doi.org/10.26599/JGSE.2023.9280020

Journal homepage: http://gwse.iheg.org.cn

Research Paper

Geothermal anomalies in the Xianshuihe area: Implications for tunnel construction along the Sichuan-Tibet Railway, China

Feng Liu[1,2,3], Wei Zhang[1,3*], Gui-ling Wang[1,3], Shuai-chao Wei[1,3], Chen Yue[1,3], Guang-zheng Jiang[4], Yu-zhong Liao[1,3]

[1] *Institute of Hydrogeology and Environmental Geology*, *Chinese Academy of Geological Science*, *Shijiazhuang* 050061, *China*.
[2] *China University of Geosciences(Beijing)*, *Beijing* 100083, *China*.
[3] *Technology Innovation Center of Geothermal & Hot Dry Rock Exploration and Development*, *Ministry of Natural Resources*, *Shijiazhuang* 050061, *China*.
[4] *Chengdu University of Technology*, *Chengdu* 610059, *China*.

Abstract: This study presents a comprehensively analysis of geothermal characteristics in the Xianshuihe geothermal area along the Sichuan-Tibet Railway, using temperature logging, temperature monitoring and thermal conductivity measurement, and regional geothermal geological survey data. The research focuses on the geothermal background, geothermal field, and their potential impact on the surrounding tunnels. The investigation reveals that the average heat flow value in the study area is approximately 73.0 mW/m^2, significantly higher than the average terrestrial heat flow in mainland China (62.5 mW/m^2). This high terrestrial heat flow signifies a distinct thermal background in the area. In addition, geothermal anomalies in the area are found to be closely associated with the distribution of hot springs along NW faults, indicating a strong control by the Xianshuihe fault zone. The study concludes that the region's favorable conditions for geothermal resources are attributed to the combination of high terrestrial heatflow background and water-conducting faults. However, these conditions also pose a potential threat of heat damage to the tunnels along the Sichuan-Tibet Railway. To evaluate the risk, the research takes into account the terrestrial heat flow, thermal conductivity of the tunnel surrounding rocks, characteristics of the regional constant temperature layer, as well as the distribution of hot springs and faults. The analysis specifically focuses on the thermal damage risk of Kangding 1$^{\#}$ tunnel and 2$^{\#}$ tunnel passing through the study area. Based on the findings, it is determined that Kangding 1$^{\#}$ tunnel and 2$^{\#}$ tunnel have relatively low risk of heat damage, as they have avoided most of the high temperature anomaly areas. However, several sections of the tunnels do traverse zones with low to medium temperatures, where surface rock temperatures can reach up to 45°C. Therefore, these regions should not be neglected during the construction and operation of the tunnel project, and mitigation measures may be necessary to address the potential heat-related challenges in the area.

Keywords: Xianshuihe geothermal zone; Terrestrial heat flow; Hot spring; Tunnel; Heat damage

Received: 11 Dec 2022/ Accepted: 12 Jun 2023/ Published: 15 Sep 2023

Introduction

The Sichuan-Tibet Railway, spanning approximately 1 543 km from Chengdu in the east to Lhasa in the west, is a crucial transportation railroad artery in southwestern China. The planned Ya'an-Linzhi section of this railway traverses the eastern Qinghai-Tibet Plateau, known for its complicated geological conditions and intensive tectonic activity (Zhang et al. 2021). Consequently, the engineering geological challenges for the planning and construction of this section are unprecedented (Cui et al. 2015; Peng et al. 2020; Yin et al. 2020). Located in the Mediterranean-Himalayan geothermal belt, this section passes through multiple large active geothermal areas (Guo et al. 2017), with

*Corresponding author: Wei Zhang, *E-mail address*: 18879003@qq.com

DOI: 10.26599/JGSE.2023.9280020

Liu F, Zhang W, Wang GL, et al. 2023. Geothermal anomalies in the Xianshuihe area: Implications for tunnel construction along the Sichuan-Tibet Railway, China. Journal of Groundwater Science and Engineering, 11(3): 237-248.

over 500 hot springs discovered in adjacent areas. Among these, 114 hot springs exhibit temperatures exceeding 60°C, with some reaching up to 97°C, indicating significant hydrothermal activity (Hu et al. 2013; Chen et al. 2014). The planned railroad section includes numerous tunnels constituting around 82% of its total length, with a maximum burial depth exceeding 2 000 m. These tunnels face potential high-temperature geothermal energy challenges, such as exposure to high-temperature hot water (steam), high-temperature rock masses, and thermal water erosion, particularly in geothermal anomalous areas with elevated geothermal background values (Rybach et al. 2003; Fan et al. 2019). By examining the contact relationship between various geothermal anomalous areas and the railway, along with the proposed tunnel distributions and surrounding geothermal geology, we can preliminarily predict the rock temperatures in the tunnels and assess the influence of high-temperature geothermal energy on the railway's infrastructure.

Recent years have witnessed substantial progress in research on the thermal damage to the tunnels along the Sichuan-Tibet Railway and its surrounding engineering. Li (2011) and Lu (2012) analyzed geothermal fields in the tunnels of different sections of the Lahsa-Rikaze Railway using methods such as geothermometer measurements and numerical simulations. Ma et al. (2021) and Wang et al. (2021) assessed the hydrochemical characteristics of geothermal water and geotemperature distributions in the eastern Himalayan syntaxis, respectively, predicting the risks of thermal damage to the Layue tunnel of the Sichuan-Tibet Railway. Recently, methods such as magnetotelluric sounding (Wang et al. 2021) and three-dimensional finite element modelling (Zhao et al. 2021) have been employed to investigate thermal damage to tunnels in western Sichuan. Despite these valuable contributions, certain shortcomings persist, such as insufficient basic data, a lack of analysis of the thermal property parameters of tunnel surrounding rocks, and the geothermal gradient calculations without considering regional terrestrial heat-flow values. All these limitations affect the accuracy of the assessment results.

The Baolingshan-Zheduoshan section of the Sichuan-Tibet Railway, passing through the Xianshuihe geothermal area, is characterized by widely distributed hot springs in vicinity and a designed maximum tunnel burial depth of approximately 1 200 m, which pose risks such as thermal water gushing and high-temperature at surrounding rocks. Thus, This study aims to comprehensively investigate the geothermal background of the Xianshuihe geothermal anomalous area and its impacts on the railway engineering. To achieve the goal, geotemperature measurements and long-term borehole monitoring data, as well as thermal conductivity tests of rocks of primary lithologies in this region and the results of regional hot spring surveys, are utilized. Furthermore, the study calculates terrestrial heat-flow values and analyzes shallow and deep geothermal fields, with the intention of providing a necessary scientific basis for the engineering planning and construction of the Sichuan-Tibet Railway.

1 Overview of regional geology

The Xianshuihe fault zone is situated in the transitional zone between the mountains at the western margin of the Sichuan Basin and the Qinghai-Tibet Plateau. Within the fault zone, the Kangding area is located, and it is characterized by several major faults, including the Yalahe, Selaha, Mugecuo, Zheduotang, and Yunongxi faults from east to west (Peng et al. 2020). The Xianshuihe fault zone, as one of the most active fault systems in China's onshore areas (Xiong et al. 2010; Bai et al. 2019), exhibits intensive fault activity and frequent earthquakes (Bai et al. 2018; Qin et al. 2021), contributing to the region's high heat flow background. Furthermore, the fault zone penetrates deep into the crust, providing pathways for hydrothermal activity, serving as a tectonic foundation for the development of hydrothermal system.

Geologically, the formation of the large Gonggashan-Zheduoshan granite pluton in the Kangding area can be attributed to three stages of magmatic activity, with the granite intrusion exhibiting parallel intrusion along the Xianshuihe Fault zone. Using the Yala and Yulin rivers as a boundary, the eastern part of the Gonggashan-Zheduoshan granite intrusion consists of the Jingningian migmatites and gneiss, while the western part comprises metamorphic rocks of the Xikang Group and the Indosinian-Yanshanian Zheduoshan granite (Bian, 2018). Other lithologies in the vicinity of the granite intrusion predominantly contain Triassic metamorphic sandstone of the Zhagu'nao Formation, interspersed with slate and phyllite. Additionally, Sporadic exposures limestones are are found in the east, and the Quaternary strata are limited to the valley zones.

Along the Xianshuihe fault zone, hot springs (groups) are distributed in a beadlike pattern (Fig. 1). These hot springs include the Yulingong (temperature: 65.9°C–89°C), Lucheng (37°C–40°C), Erdaoqiao (37°C), Reshuitang (40°C–

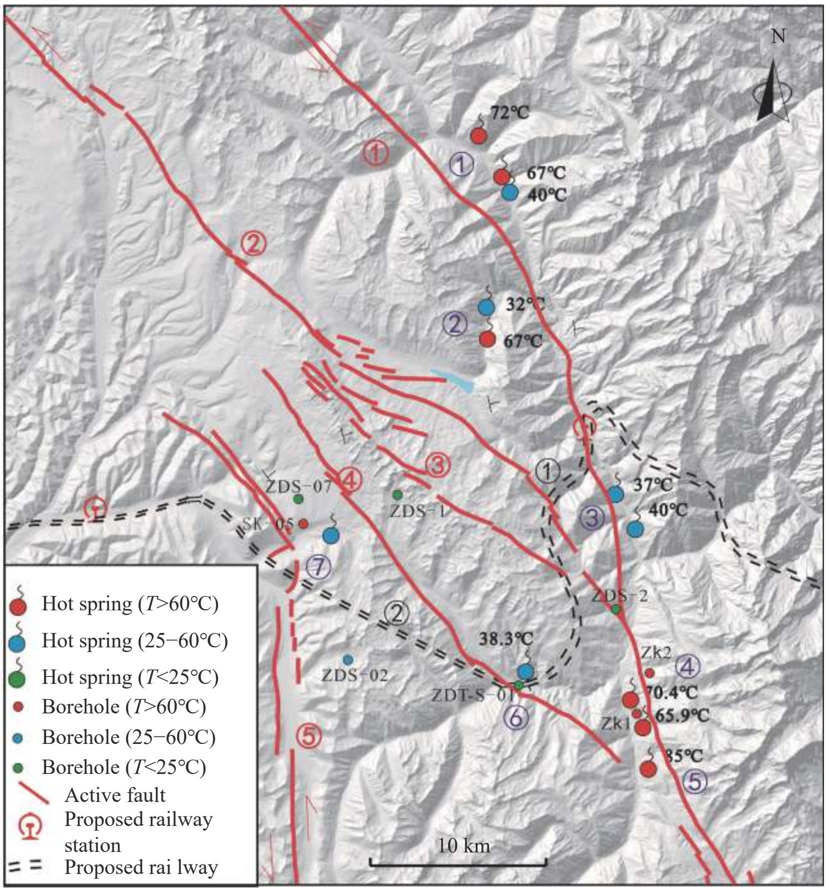

Fig. 1 Distribution of faults with geothermal activity and geothermal manifestations in the Xianshuihe fault zone

①- Zhonggu hot spring group; ②- Qisehai hot spring group; ③- Reshuitang hot spring group; ④- Erdaoqiao hot spring; ⑤- Lucheng hot spring group; ⑥- Zheduotang hot spring; ⑦- Tangniba hot spring; ①- Kangding Tunnel No. 1; ②- Kangding Tunnel No. 2; ①- Yalahe fault; ②- Selaha fault; ③- Southern Mugecuo fault; ④- Zheduotang fault; ⑤- Yunongxi fault

67°C), Qisehai (32°C–67°C), and Zhonggu hot spring groups (37°C–87°C), as well as the Zheduotang (38.5°C) and Tangniba hot spring (54°C) (Chen et al. 2014). According to the current scheme (Wang et al. 2021), Kangding Tunnel No. 1 will run from Erdaoqiao in Kangding City to Zheduotang, and Kangding Tunnel No. 2 will extend from Zheduotang to Huojiazhong, forming part of the Baolingshan-Zheduoshan section of the Sichuan-Tibet Railway the ridge-crossing scheme of the No. 3750 central line of the proposed railway (Wang et al. 2021). The zones of both tunnels intersecting with thermally and hydraulically conductive faults, along with tunnel segments with large burial depths, are susceptible to high-temperature thermal damage.

2 Regional geothermal setting

2.1 Borehole geotemperature

Geothermal logging and monitoring, as well as data collection, were conducted for multiple boreholes in the study area. Geothermal logging was performed using a SKD-3000B logging instrument, with a measurement range of 0–200°C, a resolution of 0.05°C, and a precision of ± 0.2°C. Temperature monitoring was performed using a TD-016C geothermal monitoring system, with a measurement range of 0–90°C, a resolution of 0.05°C, a precision of ± 0.2°C, and a monitoring time interval of 120 minutes. The geothermal logging was carried out after at least 48 hours of well stabilization, conforming to DZT 0181-1997 Hydrological Logging Work Specifications. For geothermal monitoring in boreholes, average temperatures of 180 days (30 days after well completion) were utilized to ensure that the measurements reached a steady or quasi-steady state (He et al. 2008).

The representative temperature curves of the study area are shown in Fig. 2, indicating significant variations in the geothermal field across the study area. As shown in Fig. 2 (a), borehole SK-ZDS-2 showed the deepest geothermal measurement and the most substantial conductive tempera-

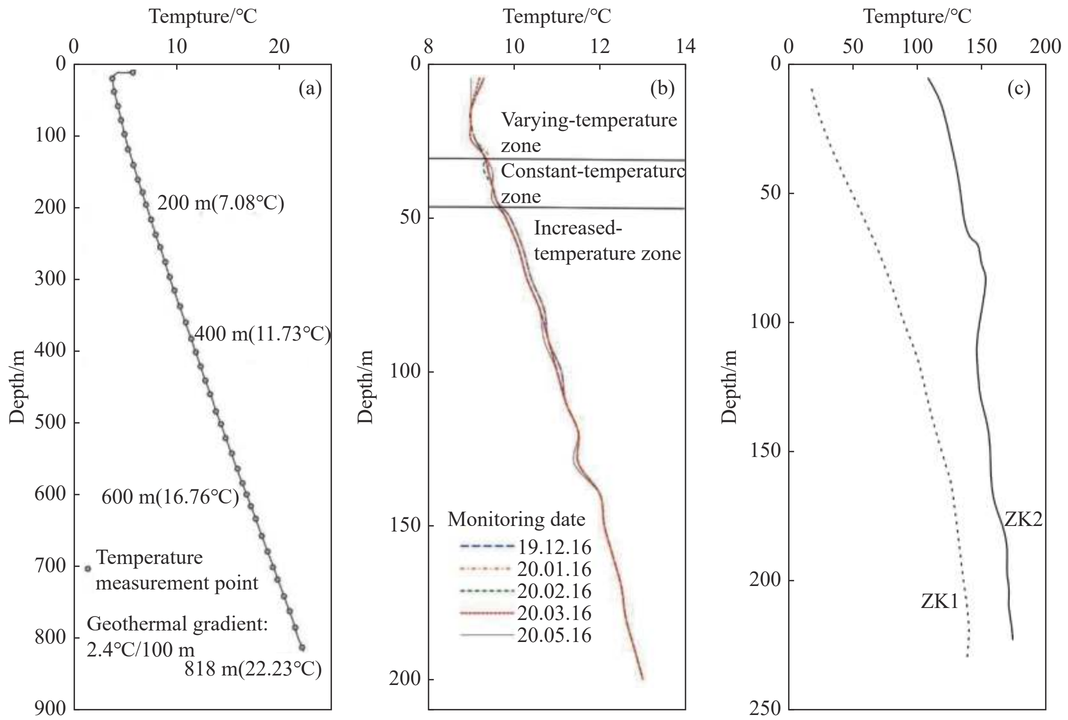

Fig. 2 Comparison between the temperature curves of representative boreholes with conductive temperature rise ((a) and (b)) and temperature curves of boreholes with convective temperature rise (c)

(a)SK-ZDS-2; (b) ZDS-02; (c) ZK1 and ZK2 (Zhang et al. 2019)

ture rise in the study area. With a geothermal gradient of about 21.3°C/km, this borehole can roughly represent the local average geothermal gradient. Fig. 2 (b) illustrates the parameters of the constant temperature zones, which were obtained through long-term geothermal monitoring. These zones have burial depths of 30–50 m and temperatures of around 9°C, slightly higher than the mean annual temperature of the study area (7°C). Borehole SK-ZDS-02 exhibited a geothermal gradient of approximately 24.2°C/km, similar to that of borehole ZDS-2, with no significant geothermal anomalies (Lin et al. 2021). These parameters serves as essential input for calculating terrestrial heat flow and predicting tunnel face temperatures in this study.

Fig. 2(c) shows that boreholes at the periphery of the hot springs in the study area mostly encounter fault zones (Zhang et al. 2019). Due to the effects of thermal water convection within these fault zones (Huang et al. 2018; Bian et al. 2018), the temperature curves of these boreholes (ZK1, ZK2) exhibit upward protrusions or minor changes, making them unsuitable for reflecting geotemperature variations in most zones of the study area. Accordingly, their temperature curves cannot be used to calculate terrestrial heat flow and tunnel face temperatures in the analysis.

Furthermore, in combination with, this study obtained the depths and bottom temperatures of several other boreholes via field investigations and data collection. As shown in Fig. 1, borehole ZDS-1 has a depth of 200 m and a bottom temperature of 4°C; borehole ZDS-07 has a depth of 212 m and a bottom temperature of 16.56°C; borehole SK-05 has a depth of 154 m and a bottom temperature of 93°C; borehole ZDT-S-1 has a depth of 128 m and a bottom temperature of 17.4°C. These boreholes, being in proximity to the proposed tunnels, can provide necessary validation data for the analysis of thermal damage to the tunnels.

2.2 Major lithologies and thermal conductivity

The examination of existing boreholes reveals distinct lithological compositions. Borehole SK-ZDS-02 is predominantly composed of squartz sandstones at depths greater than 50 m, while boreholes ZDS-1 and ZDS-2 reveal biotite granites and limestones, respectively. Thermal conductivity tests were conducted on core samples obtained from these boreholes. Furthermore, to supplement the testing data and considering the distribution of major lithologies in the study area (Liu, 2011; Ma, 2021), samples of surface rocks were collected in the vicinity of the proposed railway, including gneiss, lithic sandstones, and slates. The test results are listed in Table 1. The thermal conductivity tests were performed using an automated thermal conductivity scanner (TCS) manufactured in Germany, with a measurement range of 0.2–25 W/(m·K) and a precision of ± 3%. Among the major lithologies in the study area, quartz sandstone exhibits the widest range of thermal conductivity variation, followed by gneiss. This is likely due to variations in the cementation and crushing degrees, along with a substantial number of rok samples collected for the tests. The lithic sandstone has the highest average thermal conductivity of approximately 3.64 W/(m·K), followed by quartz sandstone and limestone. The slate exhibits the lowest thermal conductivity, with an average of around 2.2 W/(m·K). The granite and gneiss show slightly higher thermal conductivities, both below 3 W/(m·K).

Overall, the major types of rock in the study area demonstrate relatively high, with average thermal conductivities ranging from 2.20 W/(m·K) to 3.64 W/(m·K). These results indicate the ability of the rocks to efficiently conduct heat in the area.

2.3 Calculation of terrestrial heat-flow values

Regional terrestrial heat flow is a critical parameter for comprehensively characterizing the geothermal field of an area (Chen et al. 2017; Luo et al. 2019). It serves as a surface manifestation of the thermodynamic processes inside the Earth (Furlong and Chapman, 1987; Pollack et al. 1993). Thus, investigating the characteristics of regional terrestrial heat flow holds great significance in uderstanding the origin of geothermal resources and mechanisms of thermal damage (Liu et al. 2017).

This study calculated the terrestrial heat-flow values (Equation 1), based on the geothermal monitoring data from sections at depths of 50–200 m of borehole ZDS-2 (Fig. 2), the geothermal survey data from sections at depths of 100–800 m of borehole SK-ZDS-02 (Fig. 2), and the thermal conductivity test results of core samples from both boreholes.

$$Q = \Delta T / L \cdot K \tag{1}$$

Where: Q is the terrestrial heat-flow value of a well, $\Delta T/L$ is the geothermal gradient, and K is the thermal conductivity. In cases where a borehole holds multiple sections with different geothermal gradients and lithologies, the overall terrestrial heat-flow value of the borehole can be determined using a weighting method for various depth sections.

To obtain accurate terrestrial heat-flow values, it is necessary to correct the thermal conductivity of strata at different temperatures using the following Equations (2) and (3):

$$K(0) = K(25)\{1.007 + 25[0.003\,7 - 0.007\,4/K(25)]\} \tag{2}$$

$$K(T) = K(0)/\{1.007 + T[0.003\,6 - 0.007\,2/K(0)]\} \tag{3}$$

Where: T is the in situ temperature of a borehole core in degrees Celsius (°C), and $K(0)$ and $K(25)$ represnet the thermal conductivity of rocks at 0°C and 25°C, respectively, in W/(m·K). Previous studies have indicated that these correction equations are applicable to the strata with depths of several kilometers and below in China's onshore areas (He et al. 2008; Hu et al. 2015; Gong et al. 2011).

Table 2 shows that the surrounding areas of Kangding City have an average terrestrial heat-flow value of approximately 73.0 mW/m^2, which exceeds that of China's onshore areas (62.5 mW/m^2) and is comparable to that of the southeastern margin of the Qinghai-Tibet Plateau (75 mW/m^2), estimated using other indirect methods. Terrestrial heat flow is a the most accurate parameter for reflecting the geothermal field of an area (Qiu et al. 2004; Ou et al. 2004). The significantly high terrestrial heat-flow values in the study area indicate a high regional thermal background, which provides favorable geothermal geological conditions for the occurrence of geothermal resources

Table 1 Statistics of thermal conductivity of major lithologies in Xianshuihe geothermal anomalous area

Lithology	Sample quantity	Variation range of thermal conductivity / W/m·K	Mean thermal conductivity / W/m·K	Comment
Quartz sandstone	23	1.48–5.15	3.33	Core samples from SK-ZDS-02
Limestone	8	2.29–3.44	2.99	Core samples from ZDS-2
Biotite	9	2.28–2.65	2.40	Core samples from ZDS-1
Lithic sandstone	3	3.38–3.9	3.64	Surface rock samples
Slate	4	2.05–2.43	2.20	Surfaces rock samples
Gneiss	16	1.64–4.68	2.70	Surface rock samples

Table 2 Calculation results of terrestrial heat-flow values in the surroundings of Kangding City

No.	Borehole	Survey section depth/m	Geothermal gradient / °C/km	Average thermal conductivity	Terrestrial heat flow / mW/m^2	Sample quantity	Data quality
1	ZDS-2	50–200	21.3±0.21	2.99	64.7±0.6	9	A
2	SK-ZDS-02	100–800	24.0±0.05	3.33	80.0±0.2	23	A

(Liu et al. 2017). This finding aligns with the geothermal manifestation of widespread hot springs in the study area. However, the high regional thermal background values also create conducive conditions for geothermal hazards such as thermal damage to tunnels.

The temperature curves of the survey sections of the two boreholes all show fitness higher than 99%, indicating significant linear characteristics. The lengths and thermal conductivity of survey sections meet the quality criteria for Class A data (Hu et al. 2015).

3 Hot springs in the study regional

As shown in Fig. 1, several active faults have developed in the Xianshuihe fault zone. Thease faults, with their high thermal and hydraulic conductivity, primarily control the distribution of hot springs (Zhang et al. 2021) along the fault zone, where numerous fissures in the fault fracture zones and their surrounding country rocks constitute the geothermal reservoirs. The geothermal system is sustained by meteoric water and seasonal meltwater which provide sufficient feedwater to circulate through the relatively well-developed fissures in the region. After being heated by deep geothermal sources, the water ascends along the faults, forming a continuous geothermal fluid circulation system (Ma, 2021; Huang et al. 2018).

Table 3 shows the characteristics of hot springs around various faults. Among these, the Yalahe fault primarily governs the distribution of hot springs in the Yala River valley. Over 100 natural hot springs, including the Zhonggu, Reshuitang, and Erdaoqiao hot spring groups, have been identified through field surveys. These hot springs mostly have small flow rates of 0.1–0.3 L/s and temperatures of 25°C–62°C (Table 3). With the exception of the Erdaoqiao hot spring group, the remaining hot springs are located far from the proposed tunnels, thus exerting minimal influence on tunnel construction.

Along the Selaha fault, two hot springs have emerged: The Yaochi and Qisehai hot springs. Being more than 8 km away from the proposed tunnels, they have little impact on tunnel construction. The Zheduotang hot spring, exposed on the east side of the Zheduotang fault, has a temperature of 38.5°C, classified as a low-temperature hot spring. Furthermore, this hot spring is located at the exit of one proposed tunnel with a small burial depth, thus posing low risks of thermal damage in general (Xie and Yu, 2013). The Tangniba hot spring, located near the Yunongxi fault zone, has a temperature of 54°C. Boreholes in this vicinity have encountered geothermal water with a temperature of 90.3°C at the borehole bottom, which poses potential adverse effects on railway construction. Fortunately, this area is bypassed in the ridge-crossing scheme of the No. 3750 central line, thus reducing the threat of high-temperature thermal damage.

The geothermal reservoir temperatures associated with the hot springs can be estimated based on hydrochemical geothermometry. For instance, the Reshuitang and Zhonggu hot spring groups have geothermal reservoir temperatures of about 172–188°C (Bian et al. 2018) and about 122–184°C (Huang et al. 2018), respectively. Based on a geothermal gradient of 3°C/100 m (Zhang, 2012), both hot spring groups are situated at geothermal reservoir depths of approximately 3.5–6 km. Tunnels that traverse the thermally and hydraulically conductive faults below the hot springs water levels of or geothermal wells may potentially encounter geothermal water gushing (He et al. 2020).

4 Thermal damage to tunnels in the Baolingshan-Zheduoshan section of the Sichuan-Tibet railway

Fig. 3 illustrates the profile of the proposed tunnels (modified after Wang et al. 2021) in the Baolingshan-Zheduoshan railroad section, following in the ridge-crossing scheme of No. 3750 central line. Kangding Tunnels No. 1 and No. 2, Interconnected by the Zheduotang bridge, have exits at Erdaoqiao, Zheduotang, and Huojiazhong. The Kangding Tunnel No. 1 and No. 2 are approximately 17.26 km and 20.73 km long, respectively. Additionally, they have maximum and average burial depths of about 1 000 m and about 400 m (Kangding Tunnel No. 1), and about 1 250 m and about 500 m

Table 3 Characteristics of hot springs around faults in the study area

Fault	Hot spring group	Location	Elevation /m	Temperature /°C	Flow rate /L/s	Major lithology
Yalahe fault	Erdaoqiao hot spring group	Erdaoqiao of Kangding City	2 620.05	37.2	36	Late Yanshanian migmatite
	Reshuitang hot spring group	Low-lying area near the road on the opposite bank of Reshuitang in Yala Town, Kangding City.	3 014.12	25	1.35	Quartz sandstone, slate
		Reshuitang, Yala Town, Kangding City	3 018.17	44.0–45.2	0.14	Quartz sandstone, slate
		Reshuitang, Yala Town, Kangding City	3 011.25	40.2–61.3	0.19	Quartz sandstone, slate
		Reshuitang, Yala Town, Kangding City	3 048.43	46.2	0.84	Quartz sandstone, slate
	Zhonggu hot spring group	Zhonggu Village, Yala Town, Kangding City	3 074.32	37.2	0.137	Quartz sandstone, slate
		Right bank of Zhonggu Village, Yala Town, Kangding City	3 065.21	62.3	0.601	Quartz sandstone, slate
		Zhonggu Village, Yala Town, Kangding City	3 076.35	47.2	1.285	Quartz sandstone, slate
		Zhonggu Village, Yala Town, Kangding City	3 095.11	48.3	0.094	Quartz sandstone, slate
		Right bank of Yala River in Dagai Village, Yala Town, Kangding City	3 103.14	37.1	1.901	Quartz sandstone, slate
		Dagai, Yala Town, Kangding City	3 102.31	42.0–47.2	0.641	Quartz sandstone, slate
		Mouth of Xiaolongbu ravine in Dagai Village, Yala Town, Kangding City	3 109.17	25.3	0.4	Quartz sandstone, slate
		Terrace on the right bank of Yala River in Dagai Village, Yala Town, Kangding City	3 124.26	33.1–40.3	1.8	Quartz sandstone, silty slate
		Right bank of Yala River in Longbu, Dagai Village, Yala Town, Kangding City	3 214.23	29.0–32.1	2.1	Biotite granite
Selaha fault	Qisehai hot spring	Niuwogou, Kangding City	3 408	32	/	Late Yanshanian biotite granite
	Yaochi hot spring	Niuwogou, Kangding City	3 588	67	0.05	Late Yanshanian biotite granite
Zheduotang fault	Zheduotang hot spring	Zheduotang, Kangding City	3 296	38.5	/	Late Yanshanian biotite granite
Yunongxi fault	Tangniba hot spring	Tangniba, Kangding City	4 041	54	/	Late Yanshanian biotite granite

(Kangding Tunnel No. 2), respectively. Extending from east to west, both tunnels traverse several active and inactive faults in the Xianshuihe fault zone (Fig. 3). The tunnel sections intersecting with active faults and those with large burial depths may encounter high-temperature thermal damage.

In areas devoid of faults, the temperature of rock layers primarily rises through thermal conduction. The geotemperature rise predominantly depends on terrestrial heat flow and the geothermal gradient, which is depicted by the linear temperature-depth relationship as shown in Figs. 2a-b. Thus, these areas mainly exhibit a conductive temperature rise. In contrast, in areas containing hydraulically conductive faults, the temperature of rock layers is affected by the thermal convection between cold and hot water within these faults. This suggests that the geotemperature rise is primarily controlled by deep geothermal sources and thermally conductive channels, resulting in non-linear temperature-depth curves (Fig. 2c). These areas predominantly experience a convective temperature rise. Considering the variation in thermal conduction modes, it is necessary to employ different methods

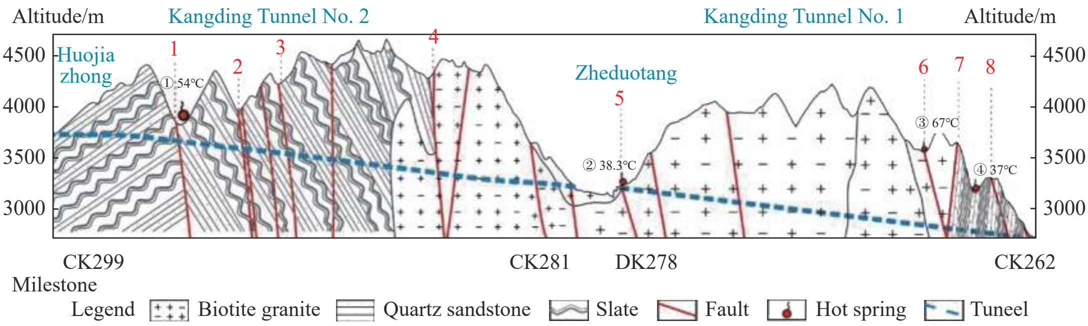

Fig. 3 Profile schematically showing the lithologies of Kangding Tunnels No. 1 and No. 2

1-Tangniba fault; 2- Yulongxi fault; 3- Huiyuan Temple-Lejipu fault; 4- Jinlong Temple-Mozigou fault; 5- Zheduotang branch fault; 6- Daxueshan-Nonggeshan fault; 7- Sandaoqiaogou fault; 8- Yalagou fault. ①- Tangniba hot spring; ②- Zheduotang hot spring; ③- Yaochi hot spring; ④-Erdaoqiao hot spring

to predict the rock temperatures of tunnels for rock layers with different temperature rise modes.

As shown in Table 3 and Fig. 3, all hot springs in the study area are located in valleys or at the foot of mountains. The elevations of tunnel faces in areas along fault that host exposed hot springs are higher than those of hot spring. Since the temperature along thermally conductive faults gradually decreases upward from deep geothermal reservoirs (Zhang, 2012), it can be inferred that the tunnel face temperatures in these areas are lower than the temperatures. However, for reliability, the temperatures of the surrounding rocks of the tunnel faces can be approximated with the temperatures of hot springs near the tunnels.

For rock layers that do not intersect faults and have no nearby hot springs, the rock temperature can be predicted using the equation for conductive temperature rise (Equation 4):

$$T = t + (H - h) \cdot gt \tag{4}$$

Where: T is the temperature of in-situ rocks at a depth of H (°C); t is the temperature of the constant temperature zone in the survey area (°C), set to 9°C according to the measured data from borehole ZDS-2; H is the depth from the surveyed rock layer to the surface (m); h is the depth from the constant temperature zone to the surface (m), set to 50 m according to the measured data from borehole ZDS-2; gt is the geothermal gradient of the area where the tunnel is located, and it can be inversely calculated using Equation 1 based on the regional terrestrial heat-flow value and the thermal conductivity of the corresponding rock layer. As shown in Fig. 4, the tunnel face predominantly comprises biotite granites, quartz sandstones, and slates. With an average terrestrial heat-flow value of about 73.0 mW/m^2, and using Equation (1) and Table 1, the regional geothermal gradients of the rock layers of biotite granites, quartz sandstones, and slates are 30.4°C/km, 21.9°C/km, and 33.2°C/km, respectively.

As a result, the isothermal map of tunnel faces was generated, using the entrance Erdaoqiao of Kanding Tunnel No. 1 (elevation: 2 730 m) as the starting point, the exit Huojiazhong of Kangding Tunnel No. 2 (elevation: 3 720 m) as the endpoint, and the tunnel faces of both tunnels as the plane. The rock temperatures of the tunnel faces were predicted, based on the burial depths, lithologies, and surrounding hot springs of the tunnels, as well as the fault distribution and temperature rise modes of various tunnel sections, as shown in Fig. 4.

According to the classification criteria for thermal damage prediction in the tunnel surveying and design stage (Xie and Yu, 2013), thermal damage to tunnels can be classified into four levels: The slightly high temperate zone (28–37°C), the moderately high temperate zone (37–50°C), the high temperate zone (50–60°C), and the ultra-high temperate zone (≥ 60°C). Based on the geotemperature calculation results, the high-temperature anomalies in the study area are shown in Fig. 4. Six high-temperature anomaly areas can be identified, with Zhonggu Village, Qisehai, Reshuitang, Lucheng, Zheduotang, and Tangniba as centers, namely the Zhonggu ultra-high-temperature anomaly area (Ⅰ), the Qisehai ultra-high-temperature anomaly area (Ⅱ), the Reshuitang moderately high-temperature anomaly area (Ⅲ), the Erdaoqiao-Lucheng ultra-high-temperature anomaly area (Ⅳ), the Zheduotang slightly high-temperature anomaly area (Ⅴ), and the Tangniba ultra-high-temperature anomaly area (Ⅵ). It is noteworthy that these high-temperature anomaly areas form a vast contiguous region without specific boundaries. Their division in this study is mainly for ease of discussion and analysis.

Kangding Tunnel No. 1 roughly avoids geothermal anomaly areas Ⅰ, Ⅱ, and Ⅳ through the

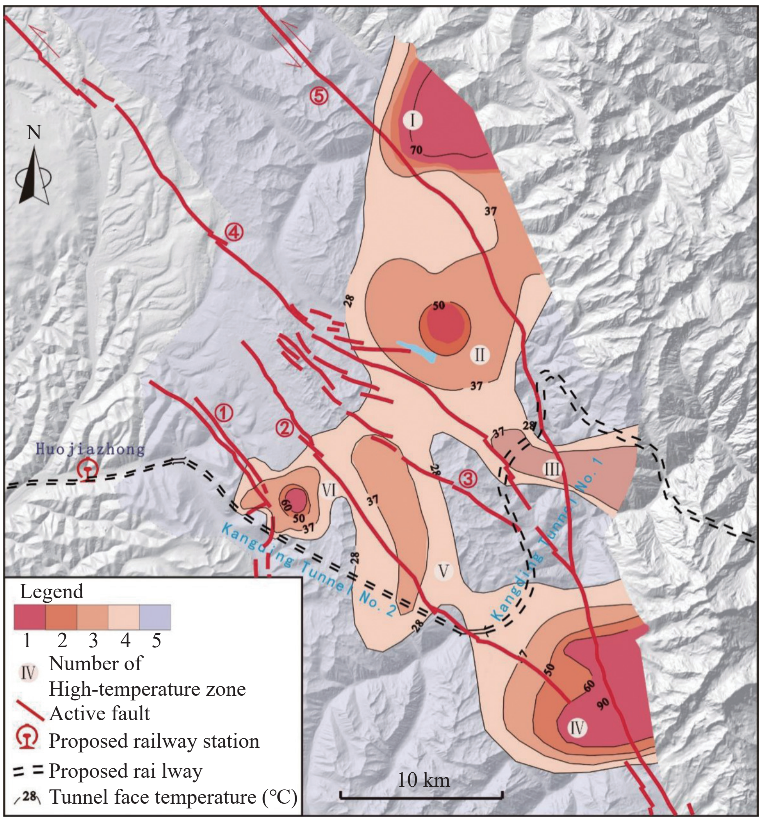

Fig. 4 Isothermal map of predicted rock temperatures for tunnel faces of Kangding Tunnels No. 1 and No. 2 of the Sichuan-Tibet Railway

1- Ultra-high-temperature zone (T > 60°C); 2- High-temperature zone (50–60°C); 3- Moderately high-temperature zone (37–50°C); 4- Slightly high-temperature zone (28–37°C); 5- Constant temperature zone (T < 28°C); ①- Yunongxi fault; ②- Zheduotang fault; ③- Southern Mugecuo fault; ④- Selaha fault; ⑤- Yalahe fault;

geological route selection, thereby reducing the risks of thermal damage. However, there are some slightly and moderately high-temperature zones at the tunnel entrance due to the presence of anomaly area Ⅲ. Additionally, some slightly high-temperature zones present at the tunnel exit due to the presence of anomaly area V, and in the middle section of the tunnel due to its considerable burial depth. It is predicted that Kangding Tunnel No. 1 includes about 9.5 km of slightly high-temperature zones and 4.3 km of moderately high-temperature zones, with a maximum rock temperature of about 42°C.

For Kangding Tunnel No. 2, the hottest part of anomaly area VI has been bypassed in the stage of route selection, greatly reducing the risk of thermal damage. However, there are multiple slightly and moderately high-temperature zones in the eastern part of the tunnel due to its substantial burial depth and at the tunnel exit due to the presence of anomaly area VI. It is predicted that Kangding Tunnel No. 2 includes about 2.2 km of slightly high-temperature zones and 2.4 km moderately high-temperature zones, with a maximum rock temperature of about 45°C.

Overall, based on existing data, the tunnel faces of Kangding Tunnels No. 1 and No. 2 mostly have normal rock temperatures through geological route planning, with only some tunnel sections including slightly and moderately high-temperature zones, which are expect to have minimal impacts on the construction and operation of the tunnels (Lu, 2012; Yin et al. 2018).

5 Conclusions and suggestions

(1) Geothermal characteristics of the Xianshuihe anomalous area

The Xianshuihe geothermal anomalous area, centered around Kangding, exhibits an average terrestrial heat-flow value of about 73.0 mW/m^2, which is significantly higher than that of China's onshore areas. This high value indicates a pronounced geothermal background in the region. The area is characterized by widespread hot springs and frequent hydrothermal activity, with the Yalahe, Selaha, Zheduotang, and Yunongxi faults within the Xianshuihe fault zone acting as major thermally and hydraulically conductive pathways for hydrothermal fluid circulation.

(2) Thermal damage risks to Kangding Tunnels No. 1 and No. 2

Kangding Tunnels No. 1 and No. 2 of the Sichuan-Tibet Railway pass through the Xianshuihe geothermal anomalous area and have maximum burial depths exceeding 1 000 m. The presence of active faults and thermal conductivity of these faults contribute to a conductive temperature rise, posing significant thermal damage risks to the tunnels. Therefore, it is necessary to carefully consider and address the potential for high-temperature thermal damage to both tunnels during the engineering and operational stages.

(3) Analysis and mitigation of thermal damage risks

This study analyzes the regional conductive temperature rise, integrating data on terrestrial heat-flow values, the thermal conductivity of the tunnels' surrounding rocks, and the parameters of the constant temperature zones. Furthermore, in junction with the analysis of convective thermal conduction of faults at the intersections of tunnels and active faults, an isothermal map is generated for the cross-section of the tunnels in the study area, identifying six high-temperature anomaly areas. The current planned routes mostly avoid these high-temperature anomaly areas through geological route selection, effectively reducing the risk of thermal damage to the tunnels. However, it is important to note that some tunnel sections remain in slightly and moderately high-temperature zones, with a maximum rock temperature at the tunnel face reaching 45°C. These sections require special attention during engineering construction and operation to mitigate potential thermal damage risks.

Overall recommendations

The Xianshuihe geothermal anomalous area is characterized by high terrestrial heat-flow values and multiple active faults, making it prone to causing high-temperature thermal damage to tunnels. Although this risk has been largely mitigated through geological route selection, several tunnel sections still remain in slightly and moderately high-temperature zones. To effective control and prevent this risk, it is necessary to identify and delineate areas at risk of high-geotemperature thermal damage. Currently, tunnel thermal damage evaluation primarily relies on preliminary analysis of borehole thermometry data, lacking a comprehensive understanding of the causes of regional thermal damage and the mechanisms of thermal and hydraulic conductivity in fault zones. Further research on the heat control and water conduction properties of regional fault zones is recommended to effectively support the evaluation of thermal damage to tunnels during the location survey stage. Improved understanding and assessment of thermal damage risks will enhance the safety and efficiency of tunnel construction and operation in the Xianshuihe geothermal anomalous area.

Acknowledgements

This study was financially supported by grants from geothermal survey project of China Geological Survey (DD221676, DD20221676-1, DD2019 0128), basic research fund Project of Chinese Academy of Geological Sciences (Research on terrestrial heat flow and thermal structure of Lithosphere in southeast China).

References

Bai MK, Chevalier ML, Pan JW, et al. 2018. Southeastward increase of the late Quaternary slip-rate of the Xianshuihe fault, eastern Tibet. Geodynamic and seismic hazard implications. Earth and Planetary Science Letters, 485: 19–31. DOI：10.1016/j.epsl.2017.12.045.

Bai YJ, Ni HY, Ge H. 2019. Advances in research on the geohazard effect of active faults on the southeastern margin of the Tibetan Plateau. Journal of Geomechanics, 25(6): 1116–1128. (in Chinese) DOI：10.12090/j.issn.1006-6616.2019.25.06.095.

Bian YY, Zhao D. 2018. Genesis of geothermal waters in the Kangding geothermal field, Sichuan Province. Acta Geoscientica Sinica, 39(4): 491–497. (in Chinese) DOI：10.3975/cagsb.2018.060401.

Chen AH, Xu X, Luo XH, et al. 2017. Heat flow characteristics and controlling factors of the Baikang Basin in South China Sea. Acta Geologica Sinica, 91(8): 1720–1728. (in Chinese) DOI：10.3969/j.issn.0001-5717.2017.08.005.

Chen YL, Zhang H, Wei YT, et al. 2014. Report of geothermal resources investigation, evaluation and regionalization in Sichuan Province. Sichuan Geological Survey Institute.

Cui P, Su FH, Zou Q, et al. 2015. Risk assessment and disaster reduction strategies for mountainous and meteorological hazards in Tibetan Plateau. Chinese Science Bulletin, 60(32):

3067−3077. (in Chinese) DOI：10.1360/N972015-00849.

Fan L. 2019. Study on the key techniques for comprehensive control of heat harm of the deep-buried and super-long tunnel with high ground temperature. Modern Tunnelling Technology, 56(6): 1−10. (in Chinese) DOI：10.13807/j.cnki.mtt.2019.06.001.

Furlong KP, Chapman DS. 1987. Thermal state of the lithosphere. Reviews of Geophysics, 25(6): 1255. DOI：10.1029/rg025i006p01255.

Gong YL, Wang LS, Liu SW, 2011. Thermal structure and thermal evolution of the Bohai Bay Basin in eastern China. Beijing: Atomic Energy Press. (in Chinese)

Guo CB, Zhang YS, Jiang LW, et al. 2017. Discussion on the environmental and engineering geological problems along the Sichuan-Tibet railway and its adjacent area. Geoscience, 31(5): 877−889. (in Chinese) DOI：10.3969/j.issn.1000-8527.2017.05.001.

He LJ, Hu SB, Huang SP, et al. 2008. Heat flow study at the Chinese Continental Scientific Drilling site: Borehole temperature, thermal conductivity, and radiogenic heat production. Journal of Geophysical Research, 113(B2): B02404. DOI：10.1029/2007jb004958.

He P, Zhang GZ, Qiang XG. 2020. Cause analysis of geothermal water and geological route selection research on the Sangzhuling tunnel of Sichuan-Tibet railway. Journal of Railway Engineering Society, 37(6): 10−13, 23. (in Chinese) DOI：10.3969/j.issn.1006-2106.2020.06.003.

Hu SB, Huang SP, 2015. Heat flow data in the continental area of China. Geothermic and its application. Beijing: Science Press. (in Chinese)

Hu XC, Fan ZC, Xie EJ, et al. 2013. Report of geothermal resources investigation, evaluation and regionalization in Tibet Autonomous Region. Geothermal Geological Team of Tibet.

Huang X, Li X, Yu ZY, et al. 2018. Thermal storage characteristics and temperature calculation in zhonggu area, Kangding. Journal of Geological Hazards and Environment Preservation, 29(4): 96−104. (in Chinese) DOI：10.3969/j.issn.1006-4362.2018.04.017.

Li JC. 2011. Research on location of geothermic tunnel of Lhasa-Rikaze railway. Journal of Railway Engineering Society, 28(4): 42−46. (in Chinese) DOI：10.3969/j.issn.1006-2106.2011.04.009.

Lin WJ, Wang GL, Shao JL, et al. 2021. Distribution and exploration of hot dry rock resources in China: Progress and inspiration. Acta Geologica Sinica, 95(5): 1366−1381. (in Chinese) DOI：10.19762/j.cnki.dizhixuebao.2021213.

Liu F, Lang XJ, Lu C, et al. 2017. Thermophysical parameters and lithospheric thermal structure in Guide Basin, Northeast Qinghai-Tibet Plateau. Environmental Earth Sciences, 76(5): 199. DOI：10.1007/s12665-017-6503-2.

Liu YM. 2011. Genesis of the geothermal water in simaqiao—Xiaoreshui area of Kangding, Sichuan Province. Beijing: China University of Geosciences. (in Chinese)

Lu D. 2012. Numerical simulation and classification on geothermal field of lasa-rikaze railway tunnels in yarlungzangbo canyon area. M. S. thesis. Chengdu: Southwest Jiaotong University. (in Chinese)

Luo L, Zhu X, He CY, et al. 2019. Study on the genesis of geothermal fluid in Xianyang geothermal field. Geological Review, 65(6): 1422−1430. (in Chinese) DOI：10.16509/j.georeview.2019.06.009.

Ma X, Fu L, Li TF, et al. 2021. Analysis of geothermal origin in eastern Himalayan syntaxis. Geoscience, 35(1): 209−219. (in Chinese) DOI：10.19657/j.geoscience.1000-8527.2021.016.

Ou XG, Jin ZM, Wang L, et al. 2004. The thermal conductivity and its anisotropy of the rock from 100-2 000 m in the main hole of the Chinese Continental Scientific Drilling: Implications for the study of the thermal structure of subduction zones. Acta Petrologica Sinica, 1: 109−118. (in Chinese) DOI：10.3969/j.issn.1000-0569.2004.01.009.

Peng JB, Cui P, Zhuang JQ. 2020. Challenges to engineering geology of Sichuan—Tibet railway. Chinese Journal of Rock Mechanics and Engineering, 39(12): 2377−2389. (in Chinese) DOI：10.13722/j.cnki.jrme.2020.0446.

Pollack HN, Hurter SJ, Johnson JR. 1993. Heat flow from the Earth's interior: Analysis of the global data set. Reviews of Geophysics, 31(3): 267. DOI：10.1029/93rg01249.

Qin YL, Wu JL, Zhan HY, et al. 2021. Discussion on the correlation between active fault and geological disaster distribution in the Ganzi area, western Sichuan Province, China. Journal of Geomechanics, 27(3): 463−474. (in Chinese) DOI：10.12090/j.issn.1006-6616.2021.27.03.042.

Qiu NS, Hu SB, He LJ, et al. 2004. Theory and Application of Research on Thermal Regime in Sedimentary Basin. Beijing: Petroleum Industry Press. (in Chinese)

Rybach L, Wilhelm J, Gorhan H. 2003. Geothermal use of tunnel waters - a Swiss speciality. International Geothermal Conference: 17−23.

Wang SR, Zhang XY, Du SH. 2021. Geothermal distribution characteristics and prediction of Layue tunnel of Sichuan-Tibet railway passing through east syntaxis. Tunnel Construction, 41(1): 100−107. (in Chinese) DOI：10.3973/j.issn.2096-4498.2021.01.011.

Wang ZW, Xu ZX. 2021. Geological line selection of Xianshuihe structural zone of Sichuan-Tibet railway. Journal of Engineering Geology, 29(02): 466−477. (in Chinese)

Xie JT, Yu YY. 2013. Grades for heat damage in high altitude tunnel engineering. Journal of Railway Engineering Society, 30(12): 69−73. (in Chinese) DOI：10.3969/j.issn.1006-2106.2013.12.015.

Xiong TY, Yao X, Zhang YS. 2010. A review on study of activity of Xianshuihe fault zone since the Holocene. Journal of Geomechanics, 16(2): 176−188. (in Chinese) DOI：10.3969/j.issn.1006-6616.2010.02.007.

Yin L, Li YX, Wang SG, et al. 2018. Prediction of rock temperature in Gaoligongshan tunnel on dali-ruili railway. Tunnel Construction, 38(10): 1637−1642. (in Chinese) DOI：10.3973/j.issn.2096-4498.2018.10.006.

Yin YP, Wang WP. 2020. A dynamic erosion plowing model of long Run-out landslides initialized at high locations. Chinese Journal of Rock Mechanics and Engineering, 39(8): 1513−1521. (in Chinese) DOI：10.13722/j.cnki.jrme.2020.0062.

Zhang W, Wang GL, Zhao JY, et al. 2021. Geochemical characteristics of medium-high temperature geothermal fluids in west Sichuan and their geological implications. Geoscience, 35(1): 188−198. DOI：10.19657/j.geoscience.1000-8527.2021.015.

Zhang X. 2012. A study of the characteristics of hot springs of low to moderate temperature in Chengde district of northern Hebei. M. S. thesis. Beijing: China University of Geosciences. (in Chinese)

Zhang ZG, Li J, Tian ZH. 2019. Investigation and evaluation of geothermal resources of shattered fractures zones in mountainous areas of Xiaoreshui, Kangding. Journal of Hebei University of Technology, 48(3): 91−96. (in Chinese) DOI：10.14081/j.cnki.hgdxb.2019.03.015.

Zhao ZH, Xu HR, Liu F, et al. 2021. Preliminary prediction of temperature field and thermal damage in Zheduoshan region along sichuan-tibet railway. Geoscience, 35(1): 180−187. (in Chinese) DOI：10.19657/j.geoscience.1000-8527.2021.022.